ÉCOLE POLYTECHNIQUE FÉDÉRALE DE LAUSANNE

Plasticity aspects of nano scale contact

by

Till Junge

in the

School of Architecture, Civil and Environmental Engineering

Doctoral School of Mechanics of Solids and Fluids

June 2010

Contents

Chapter 1

Introduction

1.1 Motivation

The history of mankind and civilisation is closely linked to the history of tribology[1] ever since early humans around 500,000 B.C. learnt to *exploit* frictional dissipation of mechanical work to light fire by rubbing sticks together [1].

The first evidence of humans learning to *reduce* friction work stems from ancient Egypt around 1880 B.C. on drawings depicting the use of sledges, wooden rollers and lubrication for the transport of large building stones [2]. About the same time, the invention of the axle perfected the principle of the use of a rolling (rather than a sliding) motion for transport. For the following millennia, tribological advances were aimed at reducing frictional losses through the use of different animal fats or vegetable oil for lubrication and the improvement of the wheel.

Tribology seized to be an engineering discipline exclusively in 1495, when Leonardo da Vinci performed the first scientific investigation of friction [1, 2], and formulated what were later called the two basic laws of friction:

1. Friction is independent of the apparent contact area.
2. Friction is proportional the normal load.

In 1699, Amontons [3][2] rediscovered these basic laws. He, and after him Coulomb (1785) and Morin (1833), [5] interpreted the friction force as the result of interlocking mechanical asperities. An illustration of this *roughness hypothesis* is shown in Figure 1.1.

[1] This account of the history of tribology concentrates mainly on *dry contact* and intentionally skips large areas of *lubricated contact* which is out of the scope of the present study.

[2] This article has been translated in English in Amontons [4].

It could explain why both *static* friction is proportional to the load and independent of the apparent contact area. However, it failed to explain the origin of *kinetic* friction. The main alternative explanation — the *adhesion hypothesis* — was rejected because it implied a proportionality between friction and contact area, which was contrary to the experimental evidence.

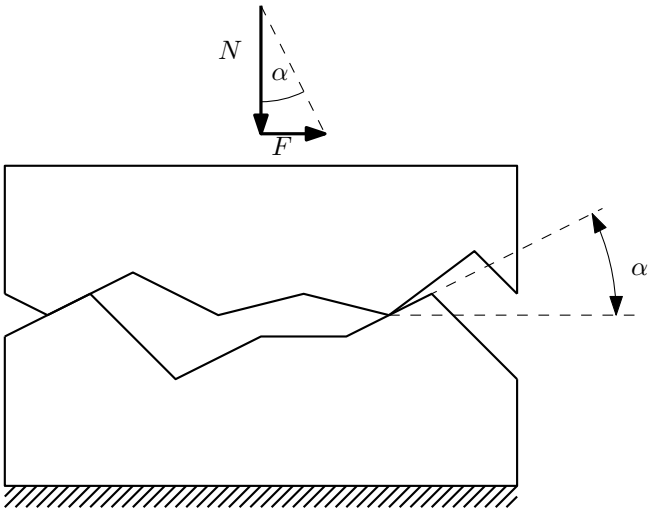

FIGURE 1.1: Roughness hypothesis: The friction force F is the force necessary to push a load N over the steepest contacting asperity slope $\tan\alpha$.

The roughness hypothesis was widely accepted until advances in surface chemistry revived the adhesion hypothesis around 1920. In 1942, Bowden and Tabor [6] introduced the important distinction between the apparent and real contact area, which allowed to explain both why friction depends on normal load but not on apparent contact area. Additionally, the distinction makes it conceptually easier to understand the often substantial difference between the static and kinetic friction coefficients, which was first clarified by Euler [2]. The definitive demise of the roughness hypothesis can be dated to 1955, when Bailey and Courtney-Pratt [7] showed that atomically smooth mica surfaces have very high friction.

When the real area of contact is taken into account, friction corresponds to the shear strength of asperity contacts [8]. This represents a substantial breakthrough in the study and understanding of friction, because for the first time it links the friction force to both the geometry and the *material properties* of the contacting bodies. Although this observation helps greatly clarify the friction mechanisms and led to more and more sophisticated friction models like, rate and state dependent friction coefficients accounting for ageing of asperity contact[3] [9], it is still impossible as of today to accurately compute friction coefficients *a priori*. Even the (macroscopic) concept of a friction coefficient itself becomes difficult to defend when applied to nano scale contacts [10].

[3] A good description of this development is given in Baumberger and Caroli [8]

It has become obvious that friction and contact are *multi scale problems* involving microscopic contacts with nanoscopic friction mechanisms. The failure of macroscopic continuum approaches to explain friction [11] calls for *multi scale methods* to understand friction and the associated wear and tear.

1.2 Objectives

This study is one of many in the general attempt of explaining and understanding friction and its consequences. It works towards the long term goal of predicting friction coefficients for macro scale contact between crystalline metals based on nano scale material and surface properties.

Friction is a phenomenon involving numerous processes (such as elasticity, plasticity, asperity locking, lattice vibrations and more) in a complicated interrelationship. It is known that friction dissipates energy in forms of plastic work and heat, yet the details are almost entirely unknown. Especially the role of plasticity is poorly investigated and most macro scale friction models do not include it, unless implicitly in the case of wear models [2, 5]. Recent molecular dynamics simulations [11] however show that mechanical contact almost always involves plasticity.

In this frame, the intermediate goal is to understand the nano and micro scale mechanisms involved in sliding friction. Our immediate goal is to develop the numerical tools necessary for the analysis of these mechanisms with a strong focus on plasticity at several length scales.

1.3 Challenges

As described in Section 1.1, the hypothesis that solids are continua can no longer be maintained at the scale of contacting asperities, and methods taking into account the discrete nature of solids are required. Micro scale plasticity for instance exhibits discontinuous behaviour due to dislocation activity [12–14] and Luan and Robbins [11] show that even properties at the atomic (nano) scale influence the way contacting asperities behave.

As long as the study is restricted to mechanical systems at reasonable temperatures without chemical reactions (i.e., systems for which the second order Born–Oppenheimer approximation [15] is satisfied) *classical molecular dynamics* (MD) are the largest-scale

method to capture contact mechanics without loss of detail. A more detailed argumentation leading to this conclusion can be found in Berendsen [16, Chapter 1] and a short description of the MD method is given in Section 2.3.

Present day computing clusters are not even close to offering the necessary computational power nor memory required for modelling entire macroscopic systems in MD. Furthermore MD requires integration time steps in the order of fs (femtoseconds) [17] which represents an important time scale restriction. The main challenge in this study is the development of suitable multi scale models which allow mixed descriptions of solids. These models should preserve the atomic scale resolution of MD where needed and at the same time reduce drastically the degrees of freedom by modelling large parts with higher scale methods such as the finite element method (FEM) or discrete dislocation dynamics (DD), described in Sections 2.1 and 2.2.

Chapter 2

State of the Art

2.1 Finite Element Method

The finite element method (FEM) is an approach to solve the equations of continuum mechanics.

In general, solids are governed by local *non-linear partial differential equations* (NLPDE). Such equations do not usually have an analytical solution and need to be linearised and discretised in both time and space in order to obtain (approximated) linear algebraic equations (LAE) which can be solved using standard linear algebra [18].

The FEM is a well established method for the spatial discretisation from NLPDE to *non-linear ordinary differential equations* (NLODE). The NLODEs can then be linearised and discretised in time using the linear iterations method (LIM) and the finite differences method (FDM) [19]. No description of the method is given here as it is a well-known and established method. For a more exhaustive description of the FEM for fully non-linear time-dependent problems refer to Curnier [19], Belytschko et al. [20] or Zienkiewicz [21], for linear time-dependent problems to Hughes [22] and for simple linear static problems to Gmür [23].

The main idea behind the FEM is the decomposition of a continuum domain into small elements for which the integral form of the governing PDE is solved approximately. FEM has classically been used for contact mechanics, however Luan and Robbins [11] showed that contact mechanics are dominated by nano scale asperities, where continuum mechanics (and therefore FEM) drastically underestimates plastic deformations. Furthermore, continuum mechanics usually fails to capture size effects, unless special theories such as strain-gradient plasticity [see 24] are used.

2.2 Discrete Dislocations Dynamics

A model that *can* capture size effects is the discrete dislocations dynamics method (DD) [14].

A dislocation is a mobile line defect in a crystal and collective dislocation motion is the mechanism of crystal plasticity [12, 25]. Two types of dislocations are depicted if Figure 2.1. Imagine to cut a half-plane (red line/plane) in the crystal and shift (slip) the layers of atoms on each side of the cut by one atom spacing against each other. Figure 2.1(a) shows a schematic of a so-called *edge dislocation*, which occurs when the slip direction is normal to the end of the cut half-plane and Figure 2.1(b) is a representation of a *screw dislocation* obtained when the slip direction is parallel to the end of the cut.

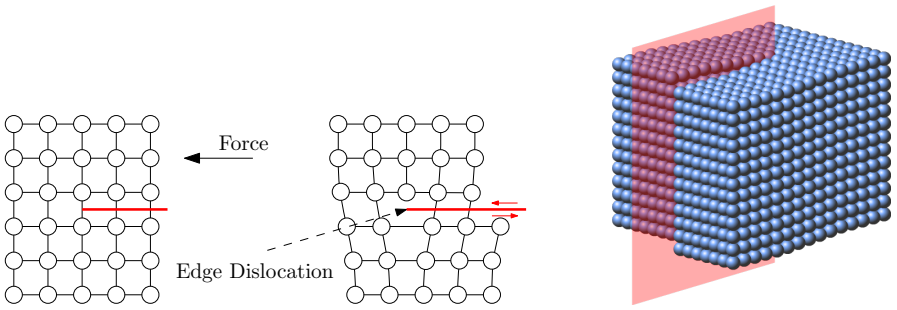

(a) Edge dislocation (b) Screw dislocation

FIGURE 2.1: Schematic representations of dislocations

In both cases the end of the cut is referred to as the dislocation line, around which the defect in the crystal structure is concentrated. Any combination between edge and screw dislocation can occur and is then called a *mixed* dislocation. The slip direction and length define the *Burgers vector* and the cut plane is called *slip-plane*. The displacement field due to a dislocation line is known for most crystal structures [12, Part 2]. The resolved shear stress in the slip plane is the driving force for dislocation mobility. For details about dislocation mobility, refer to Hirth and Jens [12, Chapter 7]. Dislocations have a stress field surrounding them which can interact with the stress fields of neighbouring dislocations. In a perfect crystal, the interactions of entangled dislocations can act as sources of new dislocations or obstacles to the motion of existing ones. Refer to Hirth and Jens [12, Chapters 5 and Part 4] for more details.

Discrete dislocation dynamics (DD) is a fairly recent method for the simulation of crystal plasticity in which dislocations are individually described as line singularities in an elastic solid. The key idea is that the discontinuous displacement fields in crystal plasticity can be computed as a superposition of the elastic response $\hat{\boldsymbol{u}}$ of the solid and

the displacement field $\tilde{\boldsymbol{u}}$ of the dislocation within the solid. That way, classic linear finite elements are used to solve the elastic field, which is then in turn used to drive the dislocations accordingly.

Both simple planar [26] and full 3D models [27] of DD exist. There is a fundamental difference between the planar and the 3D method: In two dimensions, dislocations are parallel to one another and form neither obstacles nor sources which then have to be modelled separately [13, 14, 28], whereas a fully three-dimensional simulation of dislocations forms sources and obstacles on their own [29]. Two examples of DD solvers are briefly presented here.

- **Needleman 2D [26]** Dislocation sources and obstacles are supposed to be pre-existing in the solid and distributed over a grid of slip planes. Figure 2.2(b) shows three slip plane orientations, in the complete grid, each of the slip planes is repeated periodically throughout the crystal. If a source and an obstacle lie on the same slip plane, they can interact as depicted in Figure 2.2(b). If the resolved shear stress τ on a source exceeds the nucleation stress τ_{nuc} a dipole of dislocations (two dislocations with opposite Burgers vectors) is nucleated. The position of an edge dislocation is marked with the symbol $\perp$. The nucleated dislocations then move with a velocity proportional to τ until they hit an obstacle, which they overcome if τ exceeds the obstacle strength τ_{obs}.

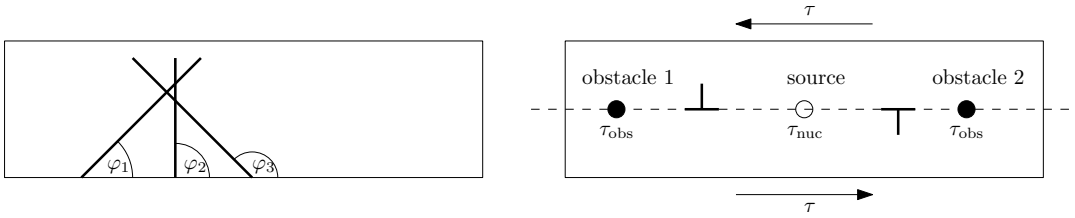

(a) Orientations of different slip systems

(b) Schematic of source-obstacle interaction

FIGURE 2.2: Planar discrete dislocation dynamics

Among others, this planar approach has been used successfully in contact mechanics [13, 28] and in the prediction of yield stress [14].

Also a 3D version based on the Needleman method has been implemented by Weygand et al. [29]

- **Cai 3D [27, 30]**
A dislocation structure is discretised in linear segments as shown if Figure 2.3. The self energy $E(\boldsymbol{r}_1, \boldsymbol{r}_2, \cdots)$ of such a discretised dislocation network is given by the elastic energy due to its displacement field [31]. The force acting on node i is obtained by derivation,

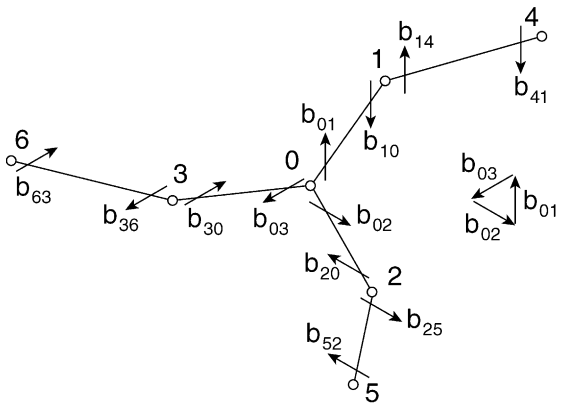

FIGURE 2.3: Dislocation network represented as a set of "nodes" interconnected by straight segments (Figure from Cai and Bulatov [30])

$$\boldsymbol{f}_i = \nabla_{\boldsymbol{r}_i} E(\boldsymbol{r}_1, \boldsymbol{r}_2, \cdots, \boldsymbol{r}_n), \tag{2.1}$$

and its velocity $\boldsymbol{v}_i$ is determined according to a constitutive law. In the example of FCC metals such a law could be a linear viscous one, e.g.,

$$\boldsymbol{v}_i = B\left(\boldsymbol{I} - \boldsymbol{n} \otimes \boldsymbol{n}\right) \boldsymbol{f}_i, \tag{2.2}$$

where B is a drag coefficient and depends on the magnitude of the Burgers vector and $\boldsymbol{n}$ is the normal unit vector of the slip plane. Note the similarity with a MD calculation scheme. The details of this method can found in Cai [32]

Such fully three-dimensional DD methods are used to predict strain hardening, among others [27, 29, 33]. A massively parallel open source implementation of this method can be found in Cai et al. [34].

The main drawback of DD methods is that dislocation nucleation is not yet fully understood [see 28]. For DD to work, dislocations must be preexisting or nucleated using ad-hoc nucleation criteria. This problem can be solved by molecular dynamics (presented in the next section), where dislocations arise naturally.

2.3 Molecular Dynamics

Classical molecular dynamics (MD) is a method to simulate matter (fluid or solid) at the atomic scale.

In MD, matter is modelled as point mass atoms subject to interatomic potentials. Born and Oppenheimer [15] formulated this approximation which is well founded if the nuclei move much slower than the electrons (i.e., in mechanics at moderate temperatures without chemical reactions). In such a case, the distribution of electrons adapts in a quasi-static manner to the positions of the nuclei, and the interatomic forces (forces between nuclei) depend only their respective positions. It can be shown that the forces are therefore conservative and derive from a potential. The force on atom i is

$$\boldsymbol{f}_i = -\nabla_{\boldsymbol{r}_i} U(\boldsymbol{r}_1, \boldsymbol{r}_2, \cdots, \boldsymbol{r}_N). \tag{2.3}$$

The equation for the evolution of a system modelled by MD is Newton's second law

$$m_i \ddot{\boldsymbol{r}}_i = \boldsymbol{f}_i. \tag{2.4}$$

Different (explicit) integration schemes such as Verlet, Leap-Frog, but also any classical mechanics integrator such as Newmark's corrector-predictor algorithm are used. More details can be found in Berendsen [16], Rapaport [17].

MD is conceptually very simple and the main difficulty in its use is the sheer size of molecular systems. As an illustration, the number N of atoms in $V = 1$ mm^3 of iron is

$$N = N_a \frac{\rho V}{m_{\text{Fe}}} \approx 8.5 \cdot 10^{19}, \tag{2.5}$$

where $N_a = 1.6022 \cdot 10^{23}$ is Avogadro's constant, ρ and m_{Fe} are the solid density and the molar mass respectively, see Table 2.1. Such a number of atoms is at least ten orders of

TABLE 2.1: Properties of iron

atomic mass	$m_{\text{Fe}} = 55.845 \ \frac{\text{g}}{\text{mol}}$
density[1]	$\rho = 7874 \ \frac{\text{kg}}{\text{m}^3}$

magnitude larger than what single computer nowadays can handle. MD relies heavily on high performance computing of parallel machines and is restricted to small simulation boxes.

Furthermore, the time steps necessary in the integration (2.4) is of the order of 1 fs $= 1 \cdot 10^{-15}$ s (femtoseconds), which is extremely small from a (contact) mechanics point of view.

2.4 Coupled Atomistics and Discrete Dislocations

The idea behind coupled atomistics and discrete dislocations (CADD) is to combine the strengths of MD and DD. The problem is cut into an MD zone and a linear elastic continuum zone. That way, only the parts of the domain in which strongly non-linear discontinuous behaviour is expected is modelled with the computationally expensive MD while the bulk of the domain is modelled with DD. CADD was first proposed by Shilkrot et al. [35] who developed it based on the quasicontinuum method [36].

Figure 2.4(a) explains the decompositions necessary for the coupling. The atomistic part is straight-forward MD. At the continuum-atomistic interface, pad (dummy) atoms on the finite elements interact with the "true"atoms, see Figure 2.4(b). The continuum part is straight-forward DD. The band of dark grey triangles in Figure 2.4(b) has a special

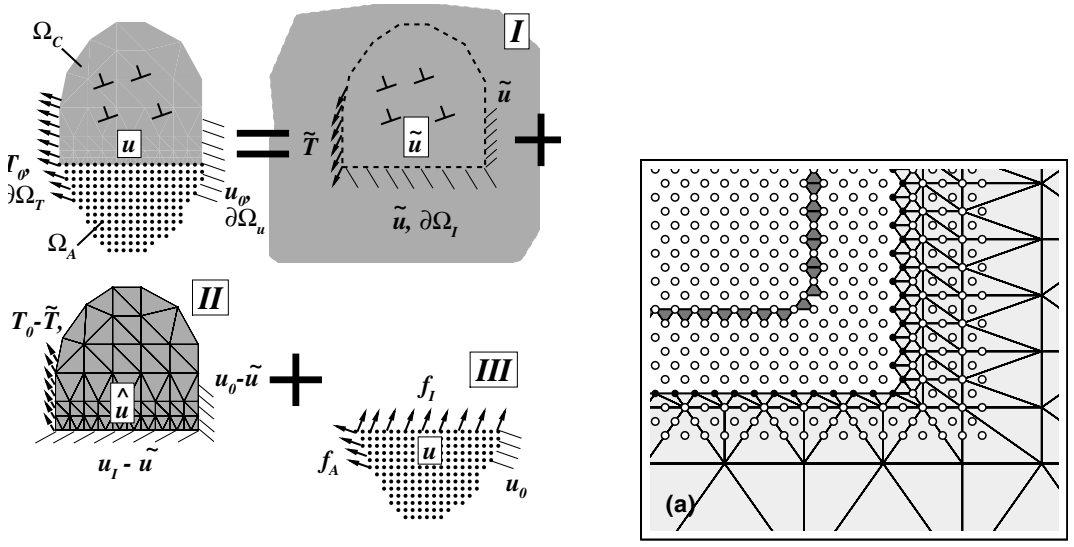

(a) Decomposition in MD and DD

(b) Close-up on interface. Continuum elements in light grey, detection band in dark grey

FIGURE 2.4: CADD decomposition of a generic domain. Figure from [35]

role, it is a detection band for dislocations: dislocations can nucleate and move within the atomistic domain. They cannot, however, move close to the interface because the discontinuity they carry with them is repulsed by the elasticity within the continuum. The detection band is sufficiently far from the interface, so dislocations reach it without being repulsed by the interface, and if one is detected, an equal discrete dislocation (same Burgers vector and slip plane) is created within the continuum a bit further down the slip plane. The slip trace of the discrete dislocation absorbs the atomistic dislocation (details in Shilkrot et al. [35]). Dislocations can effectively travel from MD to DD (and back, but not described here). This solves the main drawback of the DD method; dislocations

do not need to be explicitly nucleated within the DD zone but occur naturally in the MD zone.

So far, CADD has only been implemented in 2D, because the three-dimensional passing of dislocations between continuum and atomistics is conceptually complicated. Furthermore, a method for the automatic detection and tracking of dislocation lines in full 3D MD simulations was not available until very recently [37].

Chapter 3

Preliminary Results

This chapter describes two case studies I conducted in the first year of my PhD. They have been chosen to demonstrate the progress and preparation achieved and to underline the interest of the project.

3.1 Pure MD Nanoscratching

3.1.1 Motivation

Section 1.2 presented the study of plastic mechanisms in friction as one of the research focuses of this study. The goal of the nano scratch simulation presented in this section is to establish a method to *quantify* plastic work in friction on the simplest possible (simulated) experimental setup.

3.1.2 Simulation Setup

A single asperity nano scale scratching experiment close to absolute zero temperature is conducted in MD. Figure 3.1 shows the general setup; A spherical copper indenter (dark red atoms) scratches over a single crystal copper block. Figure 3.1 shows only one half of the system for increased visibility.

Initially, all atoms are positioned at their equilibrium lattice positions with zero initial velocity (i.e., 0 K) and the crystal orientation is such that the 111 plane is indented. Refer to Hirth and Jens [12], Weertman and Weertman [25] for more details on crystal structures. The crystal is about 570 Å long, 80 Å high and 200 Å wide, which

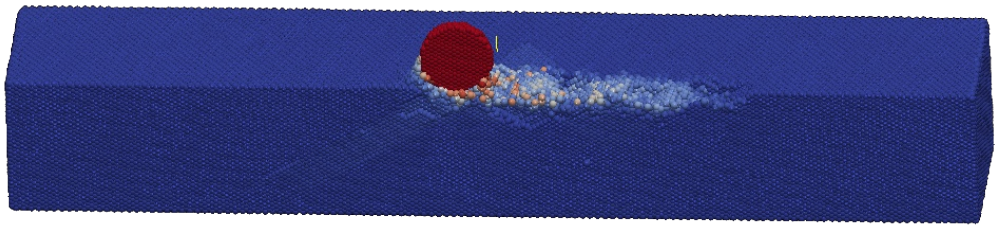

FIGURE 3.1: Nano scratch simulation

corresponds to $64 \times 16 \times 32$ lattice spacings[1]. Figure 3.2 shows the same setup as a schematic. The lowest three layers of atoms (represented by the red atoms) are held

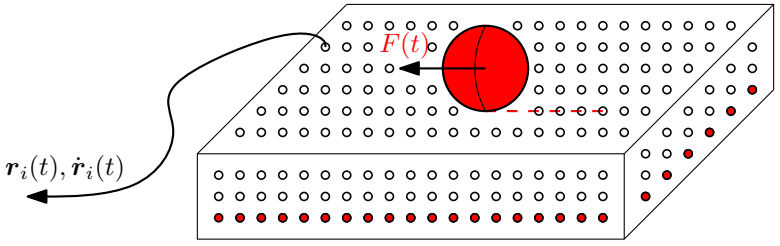

FIGURE 3.2: Simulation setup and boundary conditions

fixed and the indenter path is displacement controlled. Additionally, a thermostat layer of two atom layers thickness (not shown in the figure) just above the fixed atoms drains kinetic energy out of the system to avoid a heat buildup. Refer to Berendsen [16] for more details on thermostats. All other atoms are free to move and subject to the Mishin embedded atom model potential for copper [see 38].

For initialisation, the crystal is indented vertically to a predefined scratching depth, see Figure 3.3. For post-treatment and analysis, we evaluate the resistance force $F(t)$ on

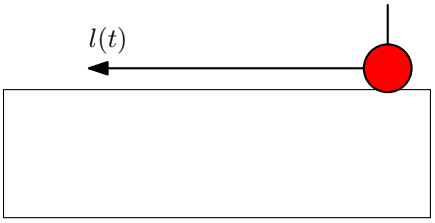

FIGURE 3.3: Indenter path

the indenter and the atomic positions $\boldsymbol{r}_i(t)$ and velocities $\dot{\boldsymbol{r}}_i(t)$ periodically and save them. Note that $F(t)$ is a scalar equal to the component of the force vector $\boldsymbol{F}(t)$ in the direction of the indenter path $l(t)$.

The simulation has been performed with a modified version of LAMMPS (Large-scale Atomistic/Molecular Massively Parallel Simulator) [see 39]. It ran on 64 Intel Xeon processors in parallel and used about 8000 processor hours per run.

[1] Note that the lattice is not cubic due to the orientation.

3.1.3 Molecular Dynamics / Molecular Statics Approach

Energy balance The only energy influx into the system is the mechanical work W provided by the scratching indenter,

$$E_{\text{in}}(t) = W(t) = \int_0^{l(t)} F(t)\ \mathrm{d}l. \tag{3.1}$$

The energy stored in the system E_{tot} is the sum of the kinetic and potential energy,

$$E_{\text{tot}}(t) = E_{\text{pot}}(t) + E_{\text{kin}}(t), \tag{3.2}$$

where E_{kin} is given by classic mechanics [see 40]

$$E_{\text{kin}}(t) = \sum_{i=1}^{N} \frac{1}{2} m_i \dot{\boldsymbol{r}}_i^2(t), \tag{3.3}$$

and the E_{pot} is given by the evaluation of the Mishin potential [see 38]

$$E_{\text{pot}}(t) = \frac{1}{2} \sum_{ij} V(r_{ij}) + \sum_i \Phi(\bar{\rho}_i), \tag{3.4}$$

where $V(r_{ij})$ is a pair potential, r_{ij} is the distance between atoms i and j, Φ is the embedding energy for an electron in the electron density $\bar{\rho}_i = \sum_{j \neq i} \rho(r_{ij})$ at the position of atom i due to all other atoms. The functions $V(r)$, $\rho(r)$ and $\Phi(\rho)$ are mathematical fitting functions without direct physical meaning.

The thermostat layer drains energy E_{out} out of the system and the amount lost is not computed in this simulation. It is only known that the layer is an energy sink

$$E_{\text{out}}(t) < 0. \tag{3.5}$$

Main idea At 0 K, a variation of E_{pot} represents elastic loading of the system or plastic deformation. After initialisation (at the end of the vertical indentation) the system is elastically loaded and this is taken to be the reference state $E_{\text{pot}}^{\text{ref}}$.

Any variation $\Delta E_{\text{pot}}(0\ \text{K})$ is then the plastic work W_{pl} in the crystal. The MD snapshots $\{\boldsymbol{r}_i, \dot{\boldsymbol{r}}_i\}\,(t)$ however are *only close to* 0 K and need to be quenched prior of evaluating ΔE_{pot},

$$E_{\text{pot}}^{\text{min}}(t) = \min_{\{\boldsymbol{r}_i(t)\}} E_{\text{pot}}(t). \tag{3.6}$$

The conjugate gradient method (CG) [41] is used for the optimisation. The evaluation of plastic work becomes

$$W_{\mathrm{pl}} = E_{\mathrm{pot}}^{\mathrm{min}}(t) - E_{\mathrm{pot}}^{\mathrm{ref}}. \tag{3.7}$$

3.1.4 Discussion of Results

Figure 3.4 shows the evolution of scratching work W and plastic work W_{pl} as functions of time for two indentation depths. The curves behave smoothly with about a quarter of the input energy ending up as plastic work. The proportion stays pretty much constant

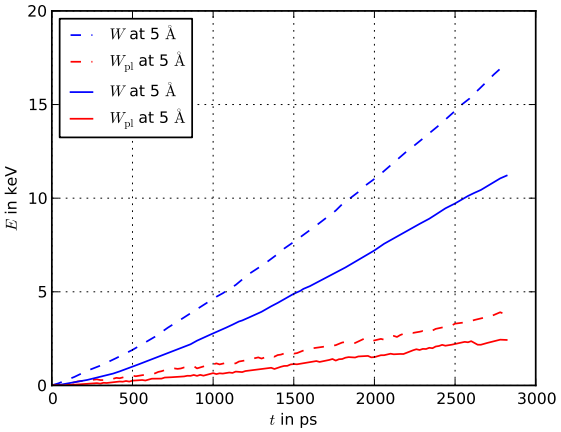

FIGURE 3.4: W and W_{pl} as functions of time for different indentation depths

for the two indentation depths. To our knowledge, there is no data available to compare these results to and validate or invalidate them. One concern is that thermal expansion of the crystal associated with the rise in temperature during scratching might change the geometry enough to violate the hypothesis of the method. The rise in temperature is shown in Figure 3.5, we can observe an increase of mere 50 K which corresponds to about 1.5‰ which is not a concern.

An idea to support the method has been borrowed from Luan and Robbins [42], where plasticity is evaluated by counting plastic events. The simple idea is to evaluate the number N_{pl} of atoms that changed their nearest neighbours during the scratch and compare them to W_{pl}. Figure 3.6 shows these comparisons for both indentation depths. In both cases, N_{pl} and W_{pl} behave very similarly. Especially the temporal coincidence of many of the spikes suggests that the way the method computes W_{pl} is closely linked to the underlying physics.

Figure 3.7 on page 18 shows a short succession of snapshots of the simulation. The atoms of the indenter are represented as red balls, the transparent dots represent atoms which are in normal crystal structure and the atoms in a disturbed neighbourhood are coloured

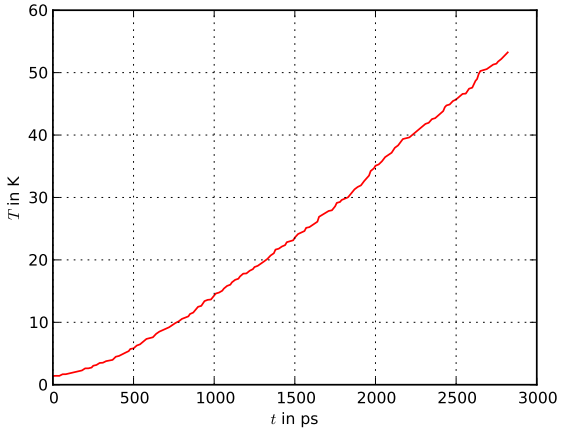

FIGURE 3.5: Temperature during scratching for 1 Å indentation depth

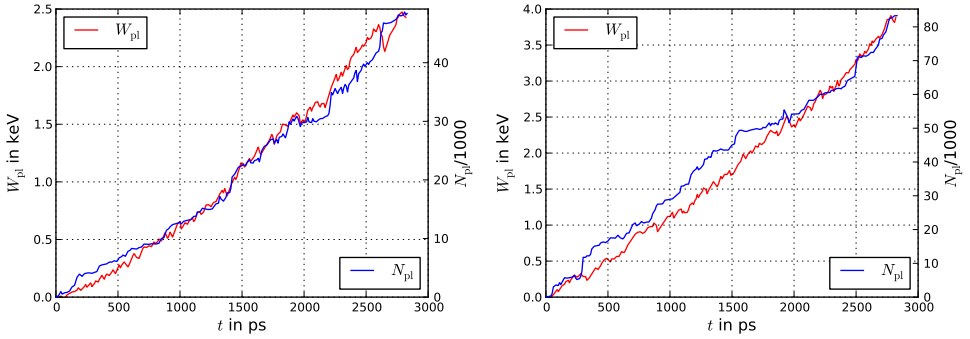

(a) 10 Å (b) 50 Å

FIGURE 3.6: Comparison between W_{pl} and N_{pl} for different indentation depths

blue. We observe two dislocation loops which have been nucleated at the surface and travelled into the crystal. The first loop is stuck at the simulation box boundary and the second loop piles up against the first one. The simulation box is too small for plasticity to develop fully. Therefore, this problem will have to be studied differently and will be readdressed in Section 4.1.

3.2 Coupled Indentation

This section presents a case study performed in collaboration with Prof. Curtin from Brown University, Providence, RI.

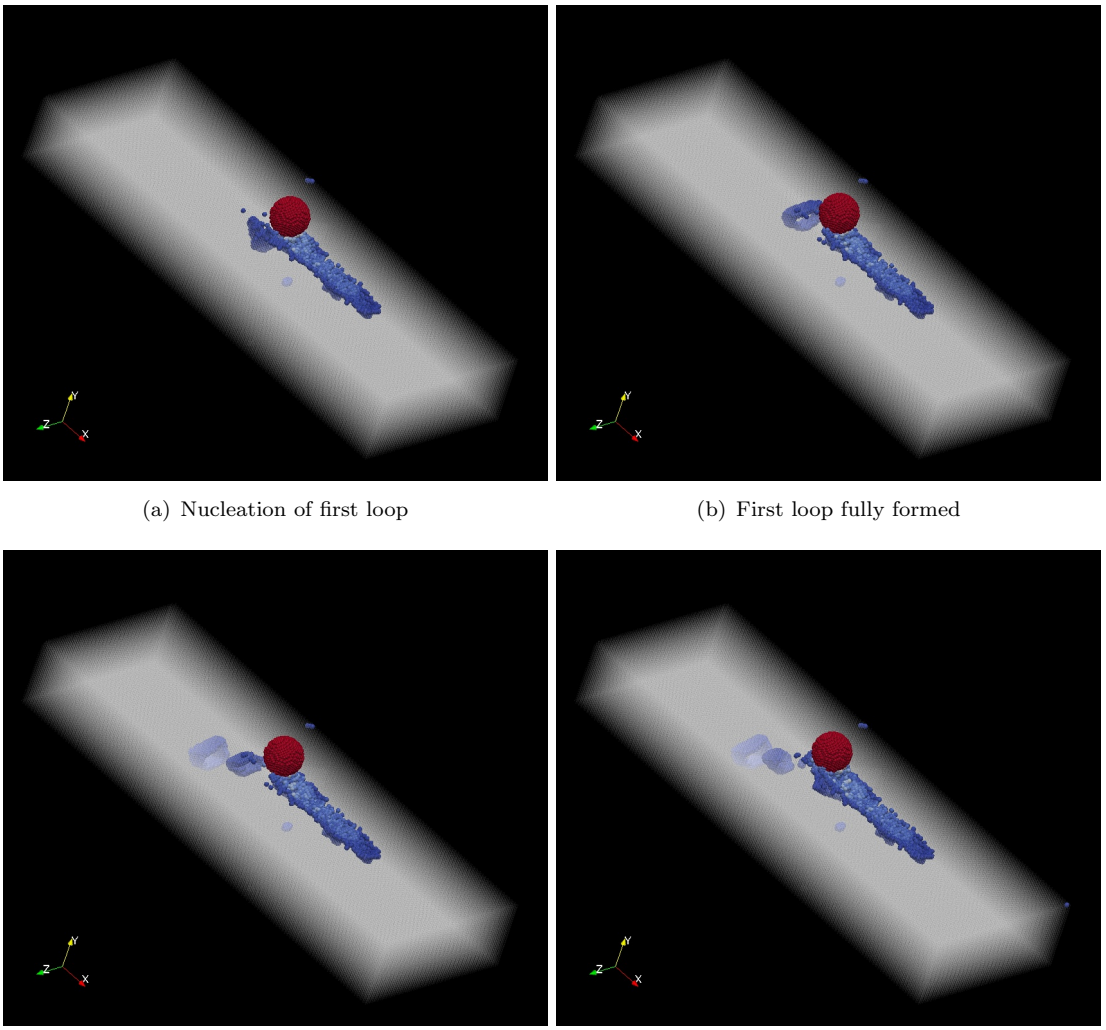

(a) Nucleation of first loop

(b) First loop fully formed

(c) Second loop nucleated, first loop travelling into the crystal

(d) Pile-up

FIGURE 3.7: Snapshot of a dislocation pattern during the simulation

3.2.1 Motivation and Setup

A simple 2D nano indentation analysis is performed to illustrate the interest of coupling MD and DD for contact problems. The goal is not so much the results but a demonstration of how much computational resources can be saved by employing multi-scale coupling methods such as CADD. Figure 3.8 shows schematically the general setup of the simulation. A rigid indenter (red) indents a single crystal of aluminium. Most of the block is modelled by static linear elastic triangular finite elements with discrete dislocations, only the part under the indenter edge — where continuum mechanics predict singular behaviour — is modelled by MD. The size of the MD box is a twentieth of the domain. Only the right part of the domain is simulated with a symmetry boundary condition of the axis of symmetry and fixed at the bottom, free on the lateral side. The top surface has an imposed displacement under the indenter and is otherwise free.

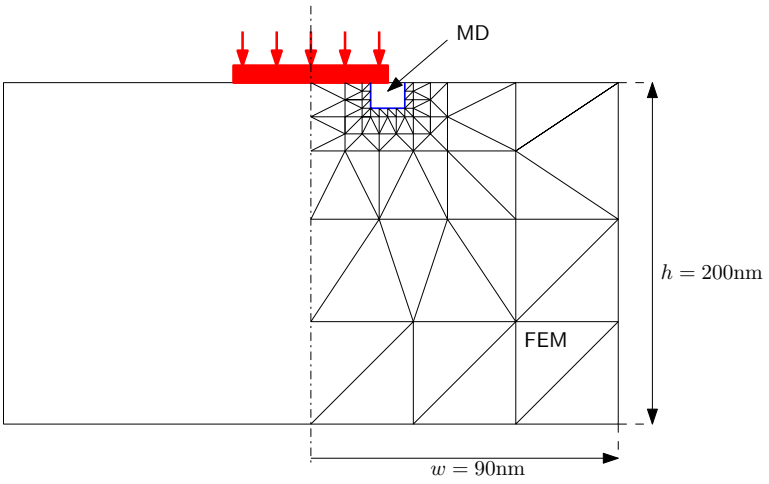

FIGURE 3.8: Nano indentation setup

The FEM part is 2D, while the MD part is so-called 2.5D; a slice of 4 lattice layers of atoms is repeated periodically the third dimension. The simulation has been performed using the CADD code developed by Shilkrot et al. [35]. It ran on a single Intel Xeon processor and used about 6 processor hours.

Note that the linear FEM calculation required the inversion of the stiffness matrix only once, its cost is, thus, negligible compared to the MD model. The speedup due to the use of CADD instead of full MD is therefore around 20.

3.2.2 Discussion of Results

Figure 3.9 shows a succession of snapshots of the simulation. Only the right symmetric part of the domain is shown. For visualisation, the atoms are treated as nodes of triangular finite elements. The elements are coloured according to averaged strain from red for zero strain to yellow for 0.01 or more average strain. The colour map has been clipped at that value in order to keep sharp dislocation lines. The black frame present in every sub-figure shows the size of the atomistic zone.

The first sub-figure shows an early snapshot when the strain concentration under the indenter edge starts to grow. In Sub-figure 3.9(b), the strain concentration has nucleated a dislocation which travels into the bulk material. Soon, in Sub-figure 3.9(c), the dislocation core reaches the vicinity of the atomistic/continuum interface where the detection band (not shown) detects it. Once detected, the dislocation is passed to the continuum. Sub-figure 3.9(d) shows the dislocation a few time steps after passing into the continuum. The position of its core is marked with a blue $\perp$ symbol. Note that the slip trace of the dislocation now extends into the continuum.

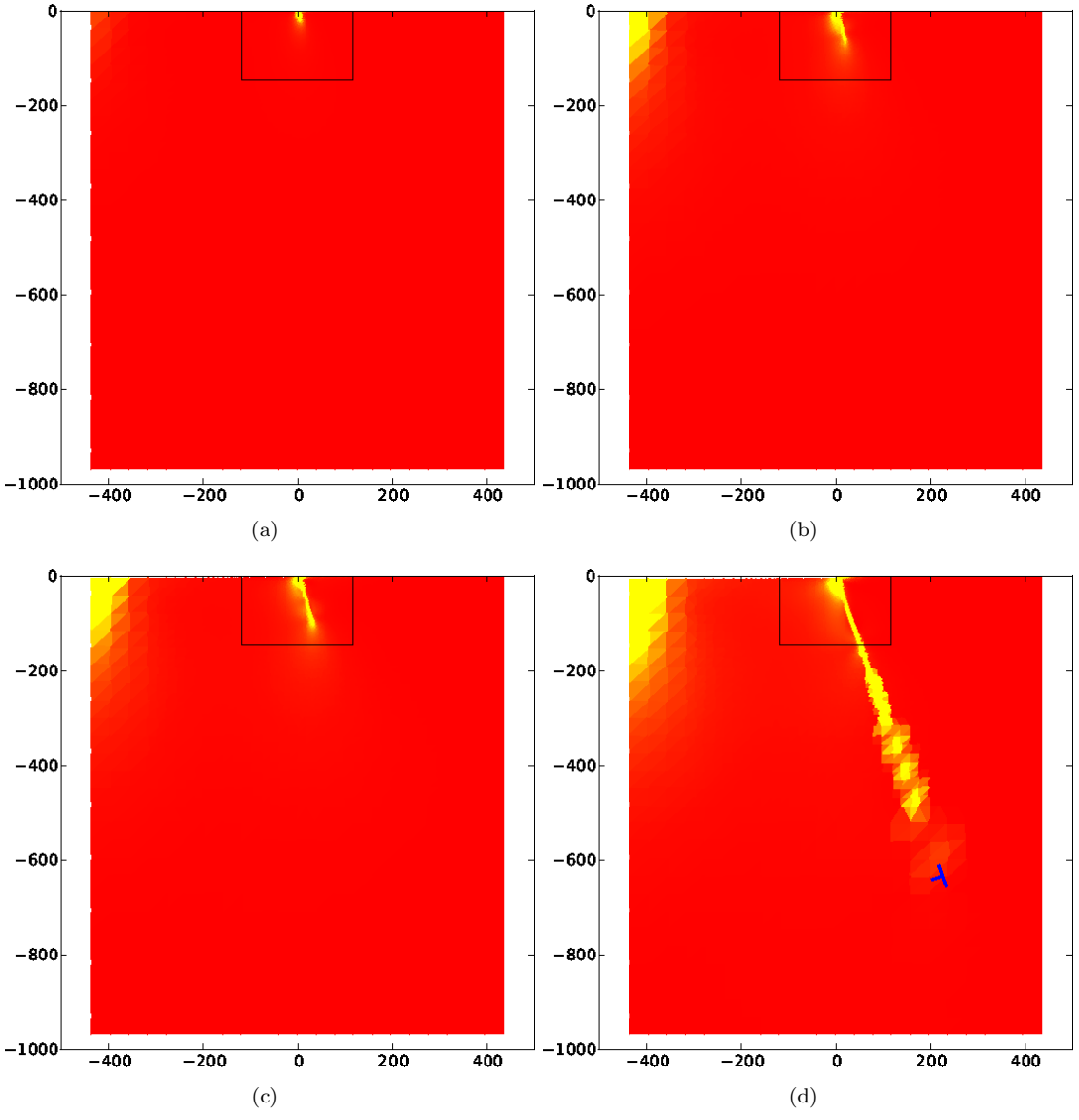

FIGURE 3.9: CADD simulation

Chapter 4

Conclusions and Outlook

4.1 Conclusions

In the previous chapter, we have presented a functional MD-based method to quantify plastic work in contact problems and demonstrated the potential of CADD-based methods to reduce computational requirements, or — reversely — increase the domain sizes at low additional computational cost.

It could be seen that the quantification of W_{pl} suffers from the limited simulation box sizes; the dislocation motion is clearly restricted, and plastic mechanisms are therefore misrepresented. The brute-force solution to this problem would be to increase the problem size. However, we established in Section 2.3 that there is no hope to solve contact problems of meaningful size (i.e., engineering-scale) anytime soon by mere MD. Furthermore, even in the small simulation presented, it is obvious that complex plastic activity is concentrated in a thin layer under the surface while plasticity in the bulk material occurs in well ordered dislocation loop, which should be dealt with using the (computationally) much cheaper DD.

The CADD simulation is an excellent example to show how much can be gained by combining the strengths of MD and DD. The drawbacks lie essentially in the fact that the only implementation is 2D only and not parallelised to run on computing clusters.

4.2 Outlook

4.2.1 CADD parallelisation and extension to 3D

As mentioned in the previous section, the implementation of CADD is its main drawback. We intend to reimplement the method in the modern framework for parallel computing Libmultiscale which is being maintained in our laboratory [see 43]. We are in an excellent position to achieve this for a set of reasons:

1. We have started a close collaboration with Prof. William A. Curtin, the author of the original CADD. He has already been a great support in using and understanding the existing CADD implementation. The road-map for the reimplementation and details about the collaboration follow below.
2. With Libmultiscale, our laboratory has a unique know-how in the implementation of parallel multi-scale methods and a substantial part of the implementation work is already accomplished.
3. Until very recently, the main obstacle to a 3D implementation of CADD was the problem of detecting dislocations in full 3D. While their detection in 2D is quite straight-forward [44], it is a quite complicated endeavour in 3D. However, in March 2010, Stukowski and Albe [37] published a method for tracking dislocation lines including their Burgers vectors on the fly during MD simulations.

In a short term, the existing 2D CADD will be replaced and allow for much larger simulations, including 2D scratching simulations which require larger MD zones than simple nano indentations. Then the 3D coupling will follow, initially without dislocation passing between continuum and atomistics. Finally the last step of passing dislocations will follow. We chose this staggered approach, because every step will yield a workable method with more capabilities than the previous one.

4.2.2 Computation of W_{pl}

4.2.2.1 Finite Temperature Extension

The way W_{pl} is computed relies heavily on the condition that the crystal is close to 0 K because of geometric changes due to thermal expansion. At finite temperature, it is an entirely open question if the 0 K reference configuration can be obtained by direct minimisation of the potential energy because we do not know how to adapt the boundary conditions during minimisation.

We intent to use a new way of computing W_{pl} inspired by the work on dislocation tracking by Stukowski and Albe [37] and the computation of dislocation network self-energy by Cai et al. [34]: The ability to track dislocations on the fly in a crystal during an MD simulation means that the self-energy of dislocation networks in MD can be computed the same way it is done in the computation of nodal forces in the 3D DD implementation of Cai et al. [27]. This way, the plastic energy can be computed at nonzero temperature.

4.2.2.2 Introduction of Micro Structure

We have obtained nano crystalline aluminium micro structures from Prof. Helena van Swygenhoven [45] at the Paul Scherrer Institute. We will apply the method to compute W_{pl} will also to them in a collaboration. Nano crystalline materials are especially interesting in the scope of this method because dislocations travel only short distances, as they are restricted by grain boundaries. This means that the simulation box size problem becomes manageable.

4.3 Detailed research plan by year

A research plan is presented with goals for each year. Everything concerning the first year is already achieved.

4.3.1 2009/2010

Goals

- Literature review on dislocations
- Literature review on MD
- Literature review on DD
- Start of a collaboration with Prof. Curtin, 10-day visit at Brown University in Providence, RI in November 2009
- Presentation of the method to compute W_{pl} at the first EPFL doctoral conference in mechanics in February 2009.
- Similar presentation at the IV European conference on computational mechanics in May 2010 [46].

Academics

A total of 10 credits have been obtained in four courses.

Course	**Teacher**	**Credits**
Mechanics of composite materials	Prof. Alain Curnier	2
Computational solid mechanics	Prof. Jean-François Molinari	2
Contact mechanics and tribology	Prof. Alain Curnier	2
Optimization and simulation	Prof. Michel Bierlaire	4

Two applied programming courses without credits :

- MPI, an introduction to parallel programming
- Python, le langage (niveau 2)

I have also been involved in three courses as a teaching assistant.

Course	**Teacher**	**Level**	**Semester**
Mécanique des solides	Prof. Alain Curnier	SGM BS6	Spring 2009
Mécanique des structures I	Dr. Eric Davalle	SGC BS3	Fall 2009
Mécanique des milieux continus	Prof. Jean-François Molinari	SGC BS2	Spring 2010

4.3.2 2010/2011

Goals

- New work visit of three weeks at Brown University in July 2010
- Reimplement 2D CADD in parallel
- Implement 3D CADD without dislocation passing
- Extend the computation of W_{pl} to finite temperature
- Publish the computation of W_{pl} with or without finite temperature extension in a journal such as Physical Review B, Acta Materialia or similar.
- Publish a second paper on the same method including micro structures in collaboration with Prof. van Swygenhoven.

Academics

I plan on visiting one more course;

Course	Teacher	Credits
Computational mechanics by reduced basis methods	Prof. Gianluigi Rozza	2

I will probably also continue being a teaching assistant in two courses;

Course	Teacher	Level
Mécanique des structures I	Dr. Eric Davalle	SGC BS3
Mécanique des milieux continus	Prof. Jean-François Molinari	SGC BS2

4.3.3 2011/2012

Goals

- Achieve dislocation passing in 3D CADD
- Publish CADD 3D in a journal such as the Journal of the Mechanics and Physics of Solids
- Publish an application paper in a journal such as Modelling and Simulation in Materials Science and Engineering
- Combine finite temperature computation of W_{pl} with CADD 3D

4.3.4 Summary of Goals

- Develop successful collaborations with
  - Prof. Helena van Swygenhoven at the Paul Scherrer Institute, Villigen
  - Prof. William Curtin at Brown University, Providence RI
- Publish 3-4 papers
- Attend 3-4 international conferences

4.4 Defense

This research proposal will be defended this coming Monday, June 28 at 10 a.m. in the conference room GC A1 416 at EPFL, see Figure 4.1 to learn how to get to there

from the main information desk. Any questions or comments are very welcome at till.junge@epfl.ch.

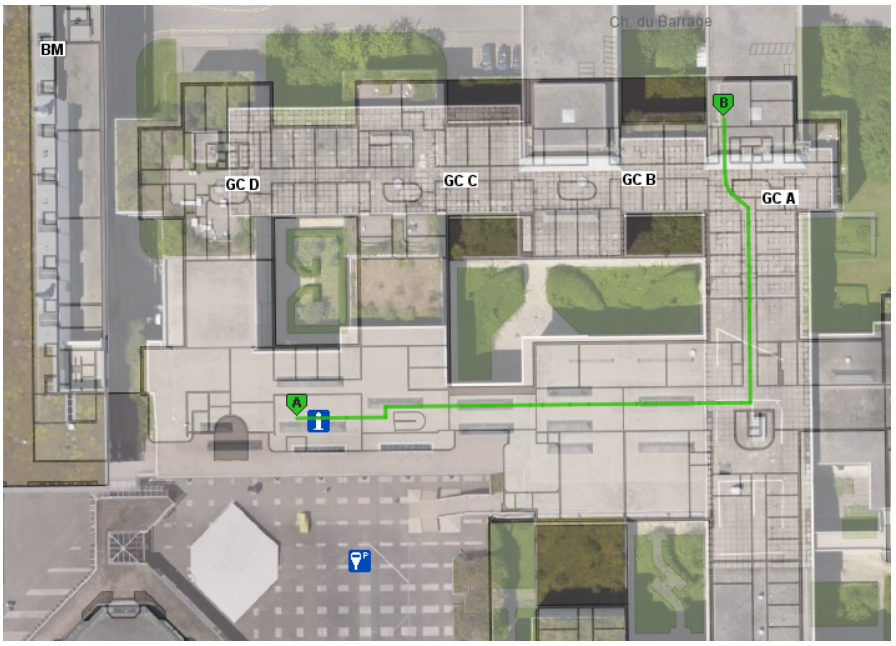

FIGURE 4.1: How to get to the defense.

Bibliography

[1] K. Carnes. The ten greatest events in tribology history. *TRIBOLOGY & LUBRICATION TECHNOLOGY*, 61(6):38–47, JUN 2005. ISSN 0024-7154.

[2] P. J. Blau. *Friction Science and Technology*. CRC Press, Boca Raton, FL, USA, 2 edition, 2008.

[3] G Amontons. Sur l'origine de la résistance dans les machines. *Mémoires de l'Académie Royale*, pages 206–222, 1699.

[4] G. Amontons. Resistance in machines. 1. Friction law. *JOURNAL OF JAPANESE SOCIETY OF TRIBOLOGISTS*, 44(4):229–235, 1999. ISSN 0915-1168.

[5] E. Rabinowicz. *Friction and Wear of Materials*. Cambridge University Press, New York, NY, USA, 1995. ISBN 0521835275.

[6] F. P. Bowden and D. Tabor. Mechanism of metallic friction. *Nature*, 150:197–199, JUL-DEC 1942. ISSN 0028-0836.

[7] A. I. Bailey and J. S. Courtney-Pratt. The Area of Real Contact and the Shear Strength of Monomolecular Layers of a Boundary Lubricant. *Proceedings of the Royal Society of London. Series A, Mathematical and Physical Sciences*, 227(1171): 500–515, 1955. ISSN 00804630. URL http://www.jstor.org/stable/99608.

[8] T. Baumberger and C. Caroli. Solid friction from stick–slip down to pinning and aging. *Advances in Physics*, 55(3-4):279, 2006. doi: {10.1080/00018730600732186}.

[9] J.-C. Gu, J. R. Rice, A. L. Ruina, and S. T. Tse. Slip motion and stability of a single degree of freedom elastic system with rate and state dependent friction. *Journal of the Mechanics and Physics of Solids*, 32(3):167–196, 1984. ISSN 0022-5096. doi: {DOI:10.1016/0022-5096(84)90007-3}. URL http://www.sciencedirect.com/science/article/B6TXB-46G2K99-8S/2/6bdeb4%c7f7cb8dd98664bbf0bdb72691.

[10] P. J. Blau. The significance and use of the friction coefficient. *Tribology International*, 34(9):585–591, 2001. ISSN 0301-679X. doi: {DOI:10.

1016/S0301-679X(01)00050-0}. URL http://www.sciencedirect.com/science/article/B6V57-43WTX9C-2/2/10a25c3%04a212ca790d2e2c21f30e76a.

[11] B. Luan and M. O. Robbins. The breakdown of continuum models for mechanical contacts. *Nature*, 435(7044):929–32, 2005. doi: {10.1038/nature03700}.

[12] John Price Hirth and Lothe Jens. *Theory of Dislocations*. Krieger Publishing Company, Malabar, Florida, U.S.A., second edition, 1992.

[13] L. Nicola, A. F. Bower, K. S. Kim, A. Needleman, and E. Van der Giessen. Multi-asperity contact: A comparison between discrete dislocation and crystal plasticity predictions. *Philosophical Magazine*, 88(30):3713, 2008. doi: {10.1080/14786430802566372}.

[14] S. S. Chakravarthy and W.A. Curtin. Effect of source and obstacle strengths on yield stress: A discrete dislocation study. *Journal of the Mechanics and Physics of Solids*, 58(5):625, MAY 2010. ISSN 0022-5096. doi: {10.1016/j.jmps.2010.03.004}.

[15] M. Born and R. Oppenheimer. Zur Quantentheorie der Molekeln. *Annalen der Physik*, 84(20):0457–0484, 1927. ISSN 0022-5096. doi: {DOI:10.1016/0022-5096(84)90007-3}.

[16] H. J. C. Berendsen. *Simulating the Physical World: Hierarchical Modeling from Quantum Mechanics to Fluid Dynamics*. Cambridge University Press, New York, NY, USA, 2007. ISBN 0521835275.

[17] D. C. Rapaport. *The Art of Molecular Dynamics Simulation*. Cambridge University Press, 2004. ISBN 0521825687.

[18] H. Anton and C. Rorres. *Elementary Linear Algebra*. Wiley, 8th Applications edition, 2000. ISBN 0471170526.

[19] A. Curnier. *Méthodes numériques en mécanique des solides*. Presses polytechniques et universitaires romandes, Lausanne, Switzerland, 2 edition, 2000.

[20] T. Belytschko, W. K. Liu, and B. Moran. *Nonlinear Finite Elements for Continua and Structures*. Wiley, 2000. ISBN 0471987743.

[21] O. C. Zienkiewicz. *The Finite Element Method*. McGraw-Hill Companies, 3 edition, 1986. ISBN 0070840725.

[22] T. J. R. Hughes. *The Finite Element Method: Linear Static and Dynamic Finite Element Analysis*. Prentice Hall, 1987. ISBN 013317025X.

[23] T. Gmür. *Méthode des éléments finis en mécanique des structures*. Presses polytechniques est universitaires romandes, Lausanne, Switzerland, 2000.

[24] A.G. Evans and J.W. Hutchinson. A critical assessment of theories of strain gradient plasticity. *Acta Materialia*, 57(5):1675, 2009. doi: {10.1016/j.actamat.2008.12.012}.

[25] J. Weertman and J.R. Weertman. *Elementary Dislocation Theory*. Oxford University Press, 1st edition, 1992.

[26] E. van der Giessen and A. Needleman. Discrete Dislocation Plasticity - A Simple Planar Model. *Modelling and simulation in Materials Science and Engineering*, 3 (5):689–735, SEP 1995. ISSN 0965-0393.

[27] W. Cai, V. V. Bulatov, T.G. Pierce, M Hiratani, M. Rhee, M. Bartelt, and M Tang. Massively-Parallel Dislocation Dynamics Simulations. *Solid Mechanics and its Applications*, 115:1, 2003.

[28] L. Nicola, A.F. Bower, K.-S. Kim, A. Needleman, and E. Van der Giessen. Surface versus bulk nucleation of dislocations during contact. *Journal of the Mechanics and Physics of Solids*, 55(6):1120, 2007. doi: {10.1016/j.jmps.2006.12.005}.

[29] D. Weygand, M. Poignant, P. Gumbsch, and O. Kraft. Three-dimensional dislocation dynamics simulation of the influence of sample size on the stress–strain behavior of fcc single-crystalline pillars. *Materials Science and Engineering: A*, 483-484:188, 2008. doi: {10.1016/j.msea.2006.09.183}.

[30] W. Cai and V. V. Bulatov. Mobility laws in dislocation dynamics simulations. *Materials Science and Engineering A*, 387-389(387-389): 277–281, 2004. ISSN 0921-5093. doi: {DOI:10.1016/j.msea.2003.12.085}. URL http://www.sciencedirect.com/science/article/B6TXD-4D04VG1-1/2/42ea160%0f44601a71e804148a05e6460. 13th International Conference on the Strength of Materials.

[31] W Cai, A Arsenlis, C Weinberger, and V Bulatov. A non-singular continuum theory of dislocations. *Journal of the Mechanics and Physics of Solids*, 54(3):561, 2006. doi: {10.1016/j.jmps.2005.09.005}.

[32] W Cai. *Atomistic and Mesoscale Modeling of Dislocation Mobility*. PhD thesis, Massachusetts Institute of Technology, Jun 2001.

[33] Vasily V Bulatov, Luke L Hsiung, Meijie Tang, Athanasios Arsenlis, Maria C Bartelt, Wei Cai, Jeff N Florando, Masato Hiratani, Moon Rhee, Gregg Hommes, Tim G Pierce, and Tomas Diaz de la Rubia. Dislocation multi-junctions and strain hardening. *Nature*, 440(7088):1174–8, 2006. doi: {10.1038/nature04658}.

[34] W. Cai, T. Arsenlis, V. Bulatov, G. Hommes, M. Rhee, and M. Tang. ParaDiS (Parallel Dislocation Simulator), -. URL http://paradis.stanford.edu. last visited June 17, 2010.

[35] L. E. Shilkrot, W. A. Curtin, and R. E. Miller. A coupled atomistic/continuum model of defects in solids. *Journal of the Mechanics and Physics of Solids*, 50(10): 2085–2106, 2002. ISSN 0022-5096. doi: {DOI:10.1016/S0022-5096(02)00017-0}. URL http://www.sciencedirect.com/science/article/B6TXB-45JGWVP-3/2/0d86525%454976036c50a79126a85c347.

[36] V. B. Shenoy, R. Miller, E. b. Tadmor, D. Rodney, R. Phillips, and M. Ortiz. An adaptive finite element approach to atomic-scale mechanics–the quasicontinuum method. *Journal of the Mechanics and Physics of Solids*, 47(3): 611–642, 1999. ISSN 0022-5096. doi: {DOI:10.1016/S0022-5096(98)00051-9}. URL http://www.sciencedirect.com/science/article/B6TXB-3VY09TR-5/2/6cec8b9%2b33d116cd65f70efd79e0228.

[37] Alexander Stukowski and Karsten Albe. Dislocation detection algorithm for atomistic simulations. *Modelling and Simulation in Materials Science and Engineering*, 18(2):025016, 2010. doi: {10.1088/0965-0393/18/2/025016}.

[38] Y. Mishin, M. Mehl, D. Papaconstantopoulos, A. Voter, and J. Kress. Structural stability and lattice defects in copper: Ab initio, tight-binding, and embedded-atom calculations. *Physical Review B*, 63(22):224106, 2001. doi: {10.1103/PhysRevB.63.224106}.

[39] *LAMMPS*, 2010. URL http://lammps.sandia.gov.

[40] Terrell L. Hill. *Statistical Mechanics: Principles and Selected Applications*. Dover Publications, 1987. ISBN 0486653900.

[41] M. Bierlaire. *Introduction à l'optimisation différentiable*. Presses Polytechniques et Universitaires Romandes, Lausanne, 2006. ISBN 2-88074-669-8. URL http://www.ppur.com/livres/2-88074-669-8.html.

[42] Binquan Luan and Mark O. Robbins. Hybrid Atomistic/Continuum Study of Contact and Friction Between Rough Solids. *Tribology Letters*, 36(1):1, 2009. doi: {10.1007/s11249-009-9453-3}.

[43] G. Anciaux. Libmultiscale. , 2009. URL http://libmultiscale.gforge.inria.fr/.

[44] R. E. Miller, L. E. Shilkrot, and W. A. Curtin. Coupled Atomistic and Discrete Dislocation Plasticity. *Phys. Rev. Lett.*, 89(2):025501, 2002.

[45] H. Van Swygenhoven, P Derlet, and A. Frøseth. Nucleation and propagation of dislocations in nanocrystalline fcc metals. *Acta Materialia*, 54(7):1975, 2006. doi: {10.1016/j.actamat.2005.12.026}.

[46] ECCOMAS. IV European Conference on Computational Mechanics. -, May 2010. URL http://www.eccm2010.org.